Atmos. Meas. Tech. Discuss., 5, 8859–8894, 2012
www.atmos-meas-tech-discuss.net/5/8859/2012/
doi:10.5194/amtd-5-8859-2012

Atmospheric Measurement Techniques Discussions

A new simplified procedure for the simultaneous SO_2 and ash retrieval in a tropospheric volcanic cloud

S. Pugnaghi[1], **L. Guerrieri**[1], **S. Corradini**[2], **L. Merucci**[2], **and B. Arvani**[1,*]

[1]Dipartimento di Scienze Chimiche e Geologiche, Università di Modena e Reggio Emilia, 41125 Modena, Italy
[2]Istituto Nazionale di Geofisica e Vulcanologia, 00143 Roma, Italy
[*]currently at: Space Science and Engineering Center, University of Wisconsin-Madison, 53706 Madison, WI, USA

Received: 26 October 2012 – Accepted: 27 November 2012 – Published: 18 December 2012

Correspondence to: S. Pugnaghi (sergio.pugnaghi@unimore.it)

Published by Copernicus Publications on behalf of the European Geosciences Union.

Abstract

A new procedure for the simultaneous estimation of SO_2 and ash abundances in a volcanic plume using thermal infrared (TIR) MODIS data is presented. Plume altitude and temperature are the only two input parameters needed to run the procedure, while surface emissivity, atmospheric profiles and radiative transfer models are not required to perform the atmospheric corrections. The proposed space-based retrievals are simple, extremely fast and can be easily extended and applied to any volcano. By linearly interpolating the radiances of the edges of the detected volcanic plume, the Volcanic Plume Removal (VPR) procedure here described, computes the radiances that would have been measured at the sensor if the plume was missing and reconstructs a new image without the plume. The comparison of the new image with the original data containing the plume highlights the plume presence and allows the computation of the plume transmittance in three TIR-MODIS bands: 29, 31 and 32 (8.6, 11.0 and 12.0 µm). The procedure results are very good when the surface under the plume is rather uniform, as it is often the case with plume widths of few tens of kilometers. As a consequence it works very well when the plume is above the sea, but still produces fairly good estimates in more challenging and not easily modeled conditions, such as images with land or uniform cloud layers under the plume. In the aforementioned bands the plume transmittances are derived in two steps: (1) using a simple model with the plume at a fixed altitude and neglecting the layer of atmosphere above it; (2) refining the first result with a polynomial relationship obtained by means of MODTRAN simulations adapted for the geographical region, the ash type and the atmospheric profiles. Bands 31 and 32 are SO_2 transparent and, from their transmittances, the ash particle effective radius (R_e) and the aerosol optical depth at 550 nm (AOD550) are computed. A simple relation between the ash transmittances of bands 31 and 29 is demonstrated and used for the SO_2 columnar content estimation. Comparing the results of the VPR procedure with the MODTRAN simulations for more than 200 thousands different cases, the frequency distribution of the differences says that: the R_e error is less than ±0.5 µm in more than

AMTD
5, 8859–8894, 2012

the 60 % of the cases; the AOD550 error is less than ±0.125 in the 80 % of the cases; the SO_2 error is less than ±0.5 g m^{-2} in more than the 60 % of the considered cases. The VPR procedure has been applied in two case studies of recent eruptions occurred at Mt. Etna volcano, Italy and successfully compared with the results obtained with the well known SO_2 and ash retrievals based look-up tables (LUTs). By recomputing the parameters of the polynomial relationship, the VPR procedure can be easily extended to other ash types and applied to different volcanoes.

1 Introduction

Worldwide volcanic activity is presently observed with an increasing variety of ground- and space-based instruments to study its influence on the Earth system either at regional and global scales. During volcanic eruptions large amounts of gases and ash can be injected into the atmosphere forming plumes and dispersed volcanic clouds. These can reside buoyant in the atmosphere and be transported downwind with a lifetime span ranging from hours to years depending on the injection height, and with scales and types of induced effects varying accordingly. The major hazard caused by volcanic ash clouds is for the aviation safety (Casadevall, 1984) and timely alert and information are needed to mitigate the risk. This kind of threat is handled by nine Volcanic Ash Advisory Centres (VAACs) around the world by providing advice on the extent and location of ash clouds to the local aviation regulators encharged to decide whether to impose air space restrictions. Satellite data collected by multispectral instruments such as MODIS aboard on the polar platforms Terra and Aqua, or the Spinning Enhanced Visible Infra Red Imager (SEVIRI) aboard on the Meteosat Second Generation (MSG) geostationary platforms play here a crucial role due to their global coverage. The most broadly used algorithms for the detection and characterization of volcanic ash clouds are based on the brightness temperature difference (BTD) in the TIR range (Prata, 1989a, b; Wen and Rose, 1994). They provide estimates maps of the volcanic

AMTD
5, 8859–8894, 2012

ash clouds' total mass, mean effective radius and aerosol optical depth (AOD) from thermal infrared (TIR) multispectral images.

Along with ash, the volcanic SO_2 emission is monitored as an important indicator of volcanic activity (e.g. Allard et al., 1994; Caltabiano et al., 1994), as an ash proxy in case of collocated SO_2 and ash clouds, and to study its impact on the climate (Robock, 2000). The SO_2 algorithm based on TIR multispectral remote sensing data was first described by Realmuto et al. (1994) for the Thermal Infrared Multispectral Scanner (TIMS) airborne sensor and exploits the SO_2 absorption feature centred at the 8.7 µm. This retrieval scheme was then successfully applied to other airborne and satellite borne multispectral imagers provided with a similar band in the TIR range including MODIS, ASTER, and SEVIRI, and later extended to the 7.3 µm SO_2 absorption feature (Pugnaghi et al., 2002; Watson et al., 2004; Prata and Kerkmann, 2007).

Further recent improvements concerned the simultaneous retrieval of SO_2 and ash. Since the volcanic ash absorbs in the whole TIR atmospheric window, its presence in the plume interferes with the SO_2 retrieval based on the 8.7 µm centred band, and to a minor extent also with 7.3 µm band retrieval. For this reason the SO_2 retrieval must be corrected for the ash contribution when both SO_2 and ash are present in the same volcanic cloud. This happens quite frequently and if the correction is not applied the SO_2 retrieval can be grossly overestimated (Corradini et al., 2009). While commonly used for SO_2 and ash clouds' quantitative retrievals these methods require a number of input parameters such as atmospheric profiles, specific volcanic ash optical properties, plume height and thickness, and make an intense use of radiation transfer codes to evaluate the atmospheric corrections look up tables (LUT). Moreover, the results have some limitations due to the assumption of a single atmospheric model over the whole plume and their reliability depends on well known conditions that must be verified on the image (Prata et al., 2001). The VPR procedure has been developed to fullfil the needs of a quick and reliable response with a potential global coverage. Its application is easy and requires only two input parameters not directly derived from the image itself, namely the plume average height and temperature, still offering reliable results.

AMTD
5, 8859–8894, 2012

The paper is organized as follows: in Sect. 2 the novel SO_2 and ash retrieval procedure is described. Sections 3 and 4 show the theoretical and experimental comparisons respectively. The latter is realized by considering two Etna eruption test cases and the results obtained have been compared with the results of the "standard" LUT retrieval approach. A sensitivity analysis related to the plume altitude is also performed. In Sect. 5 the conclusions are drafted.

2 The Volcanic Plume Removal procedure

The Volcanic Plume Removal (VPR) procedure computes, directly from the remotely sensed data, the ash and the sulfur dioxide masses contained in each pixel of a volcanic plume presents in a TIR image. After the determination of the algorithm parameters (computed once for every volcano and ash optical properties), the retrievals are realized by knowing only the volcanic cloud altitude and temperature.

The core of the procedure is the estimation of what a satellite sensor would see, if the plume would not be present; then, a simplified model of a uniform plume at a fixed altitude and temperature is applied. In the present work the multispectral radiometer MODIS on board *Terra* and *Aqua* satellites (Barnes et al., 1998; http://modis.gsfc.nasa.gov/) has been considered and the procedure has been adapted for the Mt. Etna volcano (Sicily, Italy), using specific atmospheric profiles to compute the MODTRAN simulations used to prepare the procedure. Finally, the present version of the procedure is valid only for a specific ash type (see below).

MODIS observes the Earth surface more times a day and in 36 different channels, from the visible (VIS) to thermal infrared (TIR) with a spatial resolution of 1 km at nadir in this region (TIR). Even for those channels that are well within the atmospheric windows, the radiance that reaches the sensor is always *dirtied* by the atmosphere. Therefore, precise atmospheric corrections have to be carried out to study the surface characteristics or, for example, to detect and evaluate the volcanic plume content. The possibility to easily extract useful information from the remotely sensed data itself without performing

AMTD
5, 8859–8894, 2012

complex and time consuming atmospheric corrections is of great interest for the final user. In fact, it means no need of ancillary data like the atmospheric profiles and no need of using heavy and complex software like the atmospheric radiative models. This is particularly true and desired during crisis events when a quick response is required. Clearly these advantages are partially paid with a diminished precision of the result due to the approximations introduced to simplify the procedure and reduce the computation time. Nevertheless, all the algorithms of this kind like *Split Window* (Prabhakara et al., 1974; McMillin, 1975; Price, 1984), *Dual Band* (Crisp and Baloga, 1990; Dozier, 1981), *NDVI* (Rouse et al., 1973; Roderick et al., 1996), have been obtained on these basis and their great diffusion is due to their simplicity, friendly use and fast response. The novel VPR procedure here presented has been designed with this aim: to provide an easier, faster, and reliable simultaneous retrieval of volcanic ash and SO_2 columnar abundances.

The procedure has been tested by considering MODIS images collected over Etna volcano. First it computes the radiance that the sensor would have measured if the plume would have not been present, then the plume total transmittances in the MODIS bands 29, 31 and 32 (8.6, 11.0 and 12.0 µm). Band 31 and 32 are transparent to SO_2, while band 29 is affected by both ash and SO_2 (Corradini et al., 2009). From the plume transmittances of bands 31 and 32 the ash particle effective radius (R_e) and the aerosol optical depth at 550 nm (AOD550) have been derived; knowing R_e and AOD, the ash mass can be easily computed (Wen and Rose, 1994). The band 31 plume transmittance is also used to compute the transmittance in the band 29 that is due only to the ash. This allows the estimation of the SO_2 component of the plume transmittance in the same band 29, and finally, the SO_2 columnar abundance. Let us now show in details what it has been shortly described above.

2.1 Radiance at the sensor without the plume

When a plume is present in a TIR image, it is very easy to verify the presence of a "valley" in the radiance along a line normal to the plume axis. This "valley" can change

AMTD
5, 8859–8894, 2012

its shape and characteristics according to the considered wavelength and the plume composition but it is always present.

A simple linear trend *tangent* to the two edges of the valley (i.e. the plume) gives a good estimation of the radiance at the sensor if the plume was missing. This is particularly true for a well uniform sea surface, but it works quite well even if the surface underneath the plume is the ground or a uniform cloud. Vice versa, the estimation is not so good if the two edges of the valley are above two different surfaces like: ground-sea, ground-cloud or sea-cloud. To simplify the following description we consider a common wedge shaped plume not too far from the volcano vent in a steady wind field.

The radiance at the sensor cancelling out the plume is obtained in three steps: (1) definition of a plume mask; (2) computation of the plume axis and image rotation to have the lines of the image orthogonal to the plume; (3) determination, for each line of the plume mask, of the straight line tangent to the edges of the valley (plume). The result of this process will be an image similar to the original one but without the plume.

Figure 1a shows, for the three considered MODIS bands (29, 31, 32) plus band 28 (7.3 µm): (1) the original radiance (circles) along a chosen transect normal to the plume axis. The image has been remotely sensed by MODIS *Terra* during the Mt. Etna eruption on 23 October 2011 at 21:30 UTC; underneath the plume there is the sea surface; (2) the thick coloured line is the desired radiance that would have been measured if the plume was missing; only the part inside the plume edges (the cyan vertical bars, obtained from the plume mask) has been changed, while outside the edges the original measured radiances are maintained. Therefore, after this operation, in the image with plume removed, the plume edges usually continue to be visible but, if needed this effect could be easily avoided. (3) The thin coloured line is the straight line tangent to valley (plume); to determine this straight line only the points between the blue and cyan bars are considered and only the ones satisfying a defined criterion.

A similar meaning have the lines and symbols in Fig. 1b but, in this case, another scan line normal to the plume of the same MODIS image was chosen where the left

AMTD
5, 8859–8894, 2012

edge of the plume is over the sea while the right one is over the ground (colder than the sea at 21:30 UTC). All the three bands in the atmospheric window (29, 31, 32) show this effect (difference) between the two edges. It follows that in this case the VPR procedure's results are less accurate. Vice versa, it is not present in band 28 because this band is practically not affected by the surface characteristics.

2.2 The model

The model used to determine the total transmittance in each considered band is shortly sketched in Fig. 2. The plume is located at a constant altitude Z_p, it has a constant thickness and a constant temperature T_p, i.e. the temperature of the atmosphere at the altitude Z_p. The VPR procedure requires both Z_p and T_p as input parameters. The plume altitude and temperature are clearly related but, a single data is not enough because of the seasonality. The plume transmittance is τ_p while τ' and τ'' are the atmospheric transmittances underneath and above the plume respectively. The total atmospheric transmittance when the plume is absent is: $\tau = \tau' \cdot \tau''$.

If the plume is absent, neglecting the atmospheric diffusion, the radiance at the sensor is:

$$L_0 = \left[\varepsilon \cdot B(T_s) + (1-\varepsilon) \cdot L_d\right] \cdot \tau + L_u \quad (1)$$

where ε is the surface emissivity, $B(T_s)$ is the Planck function computed at the surface temperature T_s, L_d is the atmospheric down-welling radiance and L_u is the atmospheric path or up-welling radiance. All the radiative transfer equation terms are wavelength dependent; such dependence has been omitted for clarity.

When the plume is present we assume the radiance at the sensor given by:

$$L_p = \left[\varepsilon \cdot B(T_s) + (1-\varepsilon) \cdot L_d\right] \cdot \tau \cdot \tau_p + L_u \cdot \tau_p + L_{up} = L_0 \cdot \tau_p + L_{up} \quad (2)$$

As indicated in Fig. 2, τ_p is the total plume transmittance (absorption and diffusion) and L_{up} is the path radiance due to the plume alone.

AMTD
5, 8859–8894, 2012

2.3 The Plume transmittance

In Eq. (2) it has been: (1) neglected the increase of L_d because of the presence of the plume; (2) assumed that the whole atmospheric path radiance (L_u) is attenuated by the plume transmittance τ_p, clearly this is true only for the layer underneath the plume; (3) assumed completely transparent the layer of atmosphere above the plume; that is $\tau'' = 1$. The effect of the increase of L_d is strongly reduced by the high emissivity value of the surface, in particular for the sea surface. The approximations (2) and (3) in part compensate each other and they are always more true as the plume altitude is high; that is Eq. (2) is more realistic in case of volcanic eruption than during a simple quiescent degassing.

Both the plume transmittance and the plume path radiance towards the sensor depend on absorption/emission and diffusion. It is assumed:

$$\tau_p = \tau_{pa} \cdot \tau_{pd} \tag{3}$$

where τ_{pa} is the plume transmittance due to the absorption mechanism while τ_{pd} is the plume transmittance due to diffusion by the plume particles (solid and/or liquid).

2.3.1 Absorption only

If only the absorption mechanism is present (e.g. a plume of only absorbing gases), then: $\tau_{pd} = 1$ and $\tau_p = \tau_{pa}$. In this case the radiance emitted by the plume towards the sensor is:

$$L_{up} = \varepsilon_p \cdot B(T) = (1 - \tau_p) \cdot B(T) \tag{4}$$

where ε_p is the plume emissivity; $T = T_p + \Delta T = T_p + 0.69 \cdot Z_p - 4.4$ (kelvin; with Z_p in km) is the modified plume temperature; this latter term takes into account the different thickness of the layer of atmosphere above the plume neglected by the model. This relationship has been obtained from MODTRAN simulations using the monthly mean

AMTD
5, 8859–8894, 2012

atmospheric profiles measured at Trapani (the WMO upper-air station located in the western tip of Sicily) and some reasonable altitudes for the Mt. Etna plume: 4, 6, 8 and 10 km.

From Eqs. (2) and (4), the plume transmittance can be finally calculated:

$$\tau_p = \frac{L_p - B(T)}{L_0 - B(T)} \tag{5}$$

2.3.2 Absorption and diffusion

If both absorption and diffusion mechanisms are presents (e.g. plume with gases and aerosol), then $\tau_{pd} \leq 1$. In this case the up-welling radiance due to the plume is:

$$L_{up} = \varepsilon_p \cdot B(T) = (\tau_{pd} - \tau_p) \cdot B(T) \tag{6}$$

where ε_p is the plume emissivity and T the modified plume temperature seen above.

From Eqs. (2) and (6):

$$\tau_p = \frac{L_p - \tau_{pd} \cdot B(T)}{L_0 - B(T)} \tag{7}$$

Clearly the transmittance of the ash particles due to the diffusion τ_{pd} changes according to the slant path, the size of the particles and their concentration. In this procedure the plume transmittance is computed in two steps.

First step

The first step consists in the determination of an initial raw transmittance; it is computed using only two different values of the vertical transmittance due to diffusion:

$$\tau_p' = \frac{L_p - (\tau_{pdv})^{\mu} \cdot B(T)}{L_0 - B(T)} \tag{8}$$

AMTD
5, 8859–8894, 2012

where $\tau_{pdv} = 0.965$ is the vertical plume transmittance due to diffusion and it is valid in the case of a thick plume, that is with a plume transmittance: $\tau_p^{'} \leq 0.75$; $\mu = 1/\cos\vartheta$, where ϑ is the MODIS viewing angle for the considered pixel. When the plume is more or completely transparent, that is when the pixel's transmittance computed using $\tau_{pdv} = 0.965$ is $\tau_p^{'} > 0.75$, then Eq. (8) is recomputed using $\tau_{pdv} = 0.98$. These values were empirically chosen by using MODTRAN simulations.

Second step

The second step refines the transmittance obtained in the first step using Eq. (8); it adjusts the result taking into account what not well explained by the simple model used above.

Using the ash optical properties computed from the refractive indexes tabulated by Volz (1973) many different scenarios have been simulated by means of the MODTRAN radiative transfer model. In particular have been considered: the *12* monthly mean atmospheric profiles computed by the data measured during the last 30 yr at Trapani (Sicily); it is the upper-air WMO station closest to Mt. Etna volcano; *4* plume altitudes (Z_p = 4, 6, 8, 10 km) with a constant thickness of 1 km; *11* SO_2 columnar abundances (0 to 10 g m^{-2}, step 1 g m^{-2}); *6* aerosol optical depth at 550 nm (AOD550 = 0.0, 0.078125, 0.15625, 0.3125, 0.625, 1.25); *6* effective radii (R_e = 0.785, 1.129, 1.624, 2.336, 3.360, 4.833 µm); *12* viewing angles (0 to 55 degrees, step 5 degrees) for a total of 228 096 simulations for each considered MODIS channel.

From all these simulations the radiance at the sensor when the plume is present (L_p) and the radiance without the plume (L_0) have been computed for both *Terra* and *Aqua* MODIS response functions separately. Then, knowing the plume altitude Z_p and the air temperature T_p at Z_p (from the profiles), the plume transmittances for the three considered MODIS bands 29, 31 and 32 are derived using the above described procedure. All these procedure's transmittances were then compared with the original MODTRAN transmittances and found the polynomial relationship to adjust the modelled

AMTD
5, 8859–8894, 2012

transmittances to the reference ones (that is the MODTRAN ones). Practically, the final plume transmittance is:

$$\tau_{\mathrm{p}} = \sum_{n=0}^{3} a_n \cdot (\tau_{\mathrm{p}}^{'})^n \tag{9}$$

A final control is performed on the transmittance after the second step. When the plume is very transparent, that is when the plume transmittance of band 31, computed with Eq. (9), is $\tau_{\mathrm{p},31} > 0.95$, then the total transmittance of band 29 (only) is recomputed using Eq. (5); that is, practically no ash it is assumed. Of course, it gives a small SO_2 abundance overestimation, but the procedure seems to work better.

In Table 1 are reported, for the Volz ash particles and for the three considered MODIS bands, the coefficients (a_n) of the cubic polynomial relationship of Eq. (9) estimated using all the considered scenarios. The coefficients for the two MODIS radiometers aboard *Terra* and *Aqua* satellites are slightly different because they have different spectral response functions.

Figure 3 shows for the three considered bands the *Terra* MODIS sensor (for *Aqua* it is the same) scatter plots of the MODTRAN simulated plume transmittances versus the ones computed using the described procedure. The thick straight line is the bisector. The three scatter plots show a quite good agreement.

2.4 The plume ash abundance

The total plume transmittance of the MODIS bands 31 and 32 it is assumed as due only to the ash absorption and diffusion and can be written as:

$$\tau_{\mathrm{p}} = e^{-\mu \cdot \mathrm{AOD}} \tag{10}$$

where μ takes into account the slant path and the AOD depend on the ash particles size and concentration. As can be seen in Fig. 4, that was obtained from MODTRAN

AMTD
5, 8859–8894, 2012

simulations, the AOD depends linearly on the plume AOD550 (with null offset) but with a slope m which is a function of the particle size.

$$\mathrm{AOD} = m \cdot \mathrm{AOD550} \tag{11}$$

From Eqs. (10) and (11) is clear that the ratio of the logarithms of the transmittances of band 31 and 32 computed using Eq. (9) is equal to the ratio of the slopes and therefore it is a function of the particle's effective radius too:

$$\frac{\ln(\tau_{\mathrm{p},31})}{\ln(\tau_{\mathrm{p},32})} = \frac{\mathrm{AOD}_{31}}{\mathrm{AOD}_{32}} = \frac{m_{31}}{m_{32}} \tag{12}$$

Figure 5 shows the trend of the ratio m_{31}/m_{32} and also of m_{31} versus the effective radius R_{e}. In the shown range (0.785–4.833 µm) and for the considered type of ash (Volz) they are a decreasing and an increasing monotonic function respectively. Known m_{31}/m_{32} from Eq. (12), it is possible to retrieve R_{e}, and then, from R_{e}, the slope m_{31} is also obtained; finally the AOD550, by Eq. (11), is computed.

Knowing the particle's effective radius R_{e} and the AOD550 of a pixel, the ash mass, per unit area, is computed using the Wen and Rose (1994) simplified formula:

$$M = \frac{4}{3} \cdot \left(\frac{S \cdot \rho \cdot R_{\mathrm{e}} \cdot \mathrm{AOD550}}{Q_{\mathrm{ext}}(R_{\mathrm{e}})} \right) \tag{13}$$

where S is the pixel surface, $\rho = 2.6 \times 10^3\ \mathrm{kg\,m^{-3}}$ is the density of the ash particle and $Q_{\mathrm{ext}}(R_{\mathrm{e}})$ is the extinction coefficient computed at 0.55 µm; it is a function of the effective radius R_{e}.

2.5 The plume SO_2 abundance

The total plume transmittance in the MODIS band 29 can be thought as the product of two components: (1) the ash, which attenuates the radiance both absorbing and

AMTD
5, 8859–8894, 2012

diffusing the radiation (here we consider only ash of Volz type but, of course, other ash types or other kind of aerosol particles can be present in the plume), and (2) the SO_2, whose radiance attenuation effect is only due to absorption:

$$\tau_{p,29} = \tau_{pp,29} \cdot \tau_{ps,29} \tag{14}$$

where $\tau_{pp,29}$ is the ash particle component, and $\tau_{ps,29}$ the SO_2 plume component for the MODIS channel 29. The total plume transmittance of the MODIS band 29 ($\tau_{p,29}$) is computed using Eqs. (9) or (5). Therefore, the SO_2 component ($\tau_{ps,29}$) can be derived from Eq. (14) if the particle component ($\tau_{pp,29}$) is known. It can be verified that for the Volz type aerosols the particle component of the transmittance of band 29 ($\tau_{pp,29}$) is highly correlated to the one of the band 31 ($\tau_{p,31}$) (Arvani, 2012).

Figure 6 shows this correlation; it has been obtained considering, among the above mentioned MODTRAN simulations, all the ones with no SO_2 in the plume. Therefore:

$$\tau_{pp,29} = \sum_{n=0}^{3} b_n \cdot (\tau_{p,31})^n \tag{15}$$

The polynomial fit used to get $\tau_{pp,29}$ from $\tau_{p,31}$ is a cubic here too; the b_n coefficients, for the two satellites *Terra* and *Aqua*, are reported in Table 2.

Now, from the total plume transmittance of the MODIS band 29, the only SO_2 component of the plume transmittance can be computed and then it can be derived the wanted SO_2 columnar content abundance. In fact, the SO_2 component of the plume transmittance of band 29 has been assumed to be:

$$\tau_{ps,29} = \tau_{p,29} / \tau_{pp,29} = e^{-\mu \cdot \beta_{29} \cdot c_s} \tag{16}$$

where, as usual, μ takes into account the slant path, c_s is the SO_2 columnar content abundance (in $g\,m^{-2}$) and β (in $m^2\,g^{-1}$) is: Terra: $\beta_{29} = -6.2769 \times 10^{-5} \cdot (T - T_0) + 0.0333$, Aqua: $\beta_{29} = -7.3340 \times 10^{-5} \cdot (T - T_0) + 0.0334$.

T is the previously defined: Modified Plume Temperature in K and $T_0 = 273.15\,K$. These two relationships were obtained from the MODTRAN simulations.

AMTD
5, 8859–8894, 2012

3 Theoretical comparisons

To test the theoretical part of the procedure, it has been performed a comparison between the assumed input data: the particle effective radius R_e, the aerosol optical thickness AOD550, the SO_2 columnar content c_s and the results obtained using the procedure. By means of Eq. (2) and of MODTRAN simulations 228 096 radiances at the sensor L_p have been computed assuming a constant sea surface emissivity $\varepsilon = 0.98$ and a monthly mean sea temperature. This has been computed as the monthly average temperature of a wide Mediterranean Sea region that is usually found below the Mt. Etna plume on over 30 yr of data (Arvani, 2012). For the same cases the radiances at the sensor without the plume (L_0) have also been computed. Finally, using the relationships described in the procedure the wanted results have been derived.

Figure 7 shows the distributions of the differences between the procedure results and the input values for the three input variables. It can be seen that: more than 60 % of the R_e cases have a difference lower than ±0.5 µm, about the 80 % of the AOD550 differences are lower than ±0.125, more than the 60 % of the c_s differences are lower than $\pm 0.5\,g\,m^{-2}$.

4 Experimental comparisons

The SO_2 and ash masses and fluxes retrieved from the VPR procedure have been compared with the results obtained by applying a "standard" retrieval approach based on the comparison between the measurements and the look up tables computed from radiative transfer model (LUT procedure, Corradini et al., 2009).

Two Etna eruption events have been considered for this comparison: the first was collected by MODIS-Aqua on 3 December, at 12:10 UTC during the third phase of the 2006 eruption (Andronico et al. 2009a, b), and the second event was acquired by MODIS-Terra on 23 October, at 21:30 UTC during the 2011 lava fountains activity (see Fig. 8). The 2006 event is characterized by a low SO_2 plume located at an altitude

AMTD
5, 8859–8894, 2012

of about 3.75 km (Merucci et al., 2011). The 2011 event is characterized by an higher plume altitude (about 5.5 km) and the presence of both ash and SO_2.

The standard approach uses the brightness temperature difference (BTD) applied to the MODIS channels 31 and 32 (Prata, 1989a, b; Wen and Rose, 1994; Corradini et al., 2008), to retrieve the ash parameters (AOD550, R_e and ash mass). The *chi square* procedure, applied to the MODIS channel 29, is used to retrieve SO_2 (Realmuto et al., 1994; Corradini et al., 2009, 2010). The LUT have been computed using MODTRAN code driven by the Trapani WMO atmospheric profiles closest to the two events (MODIS images) and Volz ash optical properties. The sea surface temperature has been derived from the radiative transfer equation inversion, with a constant surface emissivity equal to 0.99 (Corradini et al., 2008, 2009, 2010). The plume altitude for the 3 December 2006 derives from Andronico et al. (2009a, b), while the plume altitude for the 23 October 2011 has been evaluated from the satellite image by comparing the brightness temperature of the most opaque plume pixels with the atmospheric temperature extracted from the Trapani WMO profile (Prata and Grant, 2001; Corradini et al., 2009, 2010). The ash influence on MODIS channel 29 in the SO_2 retrieval has been corrected following the procedure described by Corradini et al. (2009).

4.1 Results

Figure 9 shows the SO_2 and ash maps and fluxes retrieved from the two MODIS images using the VPR and LUT procedures. The fluxes for the two images have been computed by multiplying the columnar abundance along a transect perpendicular to the plume axis with the wind speeds (Pugnaghi et al., 2002; Corradini et al., 2003, 2009; Theys et al., 2012). These latter, computed by interpolation from the plume altitude and the Trapani WMO wind speed profiles, are 5 and 12 m s^{-1} for the 3 December 2006 and 23 October 2011 images respectively.

The maps show the same structures and the fluxes common trends. In Table 3 the total SO_2 and ash masses and mean fluxes retrieved using the two procedures are

AMTD
5, 8859–8894, 2012

compared. All the percentage differences, computed by considering the LUT retrievals as reference, are always less than 20 % for both test cases.

4.2 Plume altitude sensitivity analysis

The main characteristic of the VPR procedure is that SO_2 and ash retrievals can be obtained from the remote sensing data itself with the only additional knowledge of the mean plume altitude and temperature. Uncertainties on these parameters clearly affect the retrieval errors. In this section a sensitivity study is carried out to investigate the SO_2 and ash total masses retrieval errors due to the altitude uncertainties. Table 4 shows the plume altitude variation considered and the corresponding plume height (Z_p) and temperature (T_p) for both the test cases. T_p temperatures have been obtained interpolating the Trapani WMO atmospheric temperature profiles of the considered days.

In Table 5 the SO_2 and ash total masses retrieved using the novel procedure with different plume altitudes and temperatures are shown. By considering an altitude uncertainty of ± 500 m, the retrieval errors lie within 15 % for the 03 December 06 event and within 33% for the 23 Octoeber 11 test case. The retrieval error increases meaningfully when the plume altitude uncertainty is ±1000 m: it becomes 30 % and 50 % for the 2006 and 2011 events respectively.

As the mean altitude decreases (and its temperature increases) the radiance emitted by the plume towards the sensor increases, and the layer of atmosphere above the plume is always less negligible. This is the reason (see Table 5) of the different variation of SO_2 and ash abundances, for the same altitude variation, according to the direction, up-wards or down-wards.

Almost the same relative variations with the plume altitude were obtained with the LUT procedure.

AMTD
5, 8859–8894, 2012

5 Conclusions

It has been described the *Volcanic Plume Removal* procedure which computes the particle effective radius, the aerosol optical depth of ash and the columnar content of both, ash and SO_2, directly from the remotely sensed data.

The used model is very simple, a plume at a constant altitude and a negligible layer of atmosphere above it. The procedure is quite independent by the surface underneath the plume if it is uniform enough. Clearly, the layer of atmosphere above the plume is always less negligible as the plume altitude decreases. Again, the plume attenuation due to the diffusion mechanisms depends on the particle size and concentration (aerosols optical depth). The proposed model accounts for these effects by using a modified plume temperature and two empirical values (one for thick plumes and one for quite transparent plumes) for the vertical plume transmittance due to the diffusion. Finally, the results are refined by means of a polynomial relationship specific for the satellite sensor, the ash type and the volcano because it is dependent from the sensor response functions, the ash optical properties and the monthly averaged atmospheric profiles of the volcanic area. The modified plume temperature and the polynomial parameters have been derived from a wide number of MODTRAN simulations.

The polynomial parameters used in this study are valid for TERRA and AQUA MODIS data (bands 29, 31 and 32 at wavelength 8.6, 11.0 and 12.0 µm respectively) collected over Mt. Etna volcano , and have been tested for the usual tropospherical plume altitudes of the Mt. Etna emissions. Moreover, they are applicable for the ash optical properties described by Volz (1973) that refer to an ash type considered typical of Mt. Etna emissions. Finally, the monthly mean profiles measured during the last 30 yr at Trapani (the WMO station closest to Mt. Etna, and located in the western tip of Sicily), have been used in the MODTRAN simulations. The parameters are written on an ancillary file and can be easily changed when recomputed for a different aerosol type (e.g. andesite) and/or sensor (e.g. SEVIRI).

AMTD
5, 8859–8894, 2012

An important part of this procedure is the relationship between the ash transmittances in bands 31 and 29; it allows the SO_2 abundance estimation from the total transmittance in band 29. The procedure works properly if only the foreseen type of ash is present. If more than one kind of particles is present in a non negligible percentage, the total effect of the aerosols is assumed due to the considered ash type only and the procedure gives erroneous results.

The comparison between the data used like input in the MODTRAN simulations and the results of the VPR procedure is quite good, but it was in part expected because the procedure has been adapted to these data while it was not so predictable the comparison between the VPR and the LUT procedures. Figure 9 shows very well the agreement between the two procedures; the maps obtained show the same structures. In particular they both show the same differences between the columnar content for SO_2 and ash emitted on 23 October 2011. The peak of SO_2 is shown at the beginning of the eruption (it is in the farthest part of the plume) while the peak of the ash is, temporally, in the final part of the phenomenon (that is, in the part of the plume closest to the vents).

As it has been shown in the last part of the paper the VPR procedure is quite sensitive to the plume altitude (and temperature). A wrong estimation of the plume altitude of 1000 m (about 7 kelv in degrees) can give an SO_2 abundance percentage difference of 50%. On the other hand, an altitude variation of 1000 m is not small for a plume at 5500 m and a usual minimum height of 3500 m (top of Mt. Etna).

It is worth to highlight that although the VPR procedure has been here described using specific case studies of Mt. Etna eruptions, it can be easily extended to any other volcano or ash type, provided the new polynomial parameters are recomputed by using local meteorological data sets and different ash optical properties.

The VPR procedure does not require atmospheric profiles nor needs the run of heavy radiative transfer codes, and the only input data needed are the plume mean altitude and temperature.

AMTD
5, 8859–8894, 2012

It is simple to apply, worldwide applicable and extremely fast, and therefore it can be very useful during crisis events when rapid responses are more valuable.

References

Allard, P., Carbonnelle, J., Metrich, N., Loyer, H., and Zettwoog, P.: Sulphur output and magma degassing budget of Stromboli volcano, Nature, 368, 326–330, 1994.

Andronico, D., Scollo, S., Cristaldi, A., and Ferrari, F.,: Monitoring the ash emission episodes at Mt. Etna: the 16th November 2006 case study, J. Volcanol. Geoth. Res., 180, 123–134. doi:10.1016/j.jvolgeores.2008.10.019, 2009a.

Andronico, D., Spinetti, C., Cristaldi, A., and Buongiorno, M.: Observations of Mt. Etna volcanic ash plumes in 2006: An integrated approach from ground-based and polar satellite NOAA-AVHRR monitoring system, J. Volcanol. Geot. Res., 180, 135–147, 2009b.

Arvani, B.: Simulazioni e modellazione della radianza delle bande termiche del MODIS per il controllo del rischio vulcanico dell'Etna, Degree in Physics Thesis at the University of Modena and Reggio Emilia, Italy, 227 pp., 2012.

Barnes, W. L., Pagano, T. S., and Salomonson, V. V.: Prelaunch characteristics of the Moderate Resolution Imaging Spectroradiometer (MODIS) on EOS-AM1, IEEE T. Geosci. Remote, 36, 1088–1100, 1998.

Caltabiano, T., Romano, R., and Budetta, G.: SO_2 flux measurements at Mount Etna (Sicily), J. Geophys. Res., 99, 12809–12819, 1994.

Casadevall, T. J.: The 1989–1990 eruption of Redoubt Volcano, Alaska: impacts on aircraft operations, J. Volcanol. Geot. Res., 62, 301–316, 1994.

Corradini, S., Pugnaghi, S., Teggi, S., Buongiorno, M. F., Bogliolo, M. P.: Will ASTER see the Etna SO_2 plume?, Int. J. Remote Sens., 24, 1207–1218, 2003.

Corradini, S., Spinetti, C., Carboni, E., Tirelli, C., Buongiorno, M. F., Pugnaghi, S., and Gangale, G.: Mt. Etna tropospheric ash retrieval and sensitivity analysis using Moderate Resolution Imaging Spectroradiometer measurements, J. Appl. Remote Ssns., 2, 023550, doi:10.1117/1.3046674, 2008.

Corradini, S., Merucci, L., and Prata, A. J.: Retrieval of SO_2 from thermal infrared satellite measurements: correction procedures for the effects of volcanic ash, Atmos. Meas. Tech., 2, 177–191, doi:10.5194/amt-2-177-2009, 2009.

AMTD
5, 8859–8894, 2012

Corradini, S., Merucci, L., Prata, A. J., and Piscini, A.: Volcanic ash and SO_2 in the 2008 Kasatochi eruption: retrievals comparison from different IR satellite sensors, J. Geophys. Res., 115, D00L21, doi:10.1029/2009JD013634, 2010.

Crisp, J. and Baloga, S.: A model for lava flows with two thermal componets, J. Geophys. Res., 95, 1255–1270, 1990.

Dozier, J.: A method for satellite identification of surface temperature fields of subpixel resolution, Remote Sens. Environ., 11, 221–229, 1981.

McMillin, L. M.: Estimation of sea surface temperatures from two infrared window measurements with different absorption, J. Geophys. Res., 36, 5113–5117, 1975.

Merucci, L., Burton, M., Corradini, S., and Salerno, G.: Reconstruction of SO_2 flux emission chronology from space-based measurements, J. Volcanol. Geot. Res., 206, 80–87, doi:10.1016/j.jvolgeores.2011.07.002, 2011.

Prabhakara, C., Dalu, G., and Kunde, V. G.: Estimation of sea temperature from remote sensing in the 11- to 13-µm window region, J. Geophys. Res., 79, 5039–5044, 1974.

Prata, A. J.: Observations of volcanic ash clouds in the 10–12 µm window using AVHRR/2 data, Int. J. Remote Sens., 10, 751–761, 1989a.

Prata, A. J.: Infrared Radiative Transfer Calculations for Volcanic Ash Clouds, Geophys. Res. Lett., 16, 1293–1296, 1989b.

Prata, A. J. and Grant, I. F.: Determination of mass loadings and plume heights of volcanic ash clouds from satellite data, CSIRO Atmospheric Research Technical Papers No. no. 48, CSIRO Marine and Atmospheric Research, 2001.

Prata, A. J. and Kerkmann, J.: Simultaneous retrieval of volcanic ash and SO_2 using MSG-SEVIRI measurements, Geophys. Res. Lett., 34, L05813, doi:10.1029/2006GL028691, 2007.

Prata, F., Bluth, G., Rose, B., Schneider, D., and Tupper, A.: Comments on "Failures in detecting volcanic ash from a satellite-based technique", Remote Sens. Environ., 78, 341–346, 2001.

Price, J. C.: Land surface temperature measurements from the split window channels of the NOAA 7 Advanced Very High Resolution Radiometer, J. Geophys. Res., 89, 7231–7237, 1984.

Pugnaghi, S., Teggi, S., Corradini, S., Buongiorno, M. F., Merucci, L., and Bogliolo, M. P.: Estimation of SO_2 abundance in the eruption plume of Mt. Etna using two MIVIS thermal infrared channels: a case study from the Sicily-1997 Campaign, B. Volcanol., 64, 328–337, 2002.

AMTD
5, 8859–8894, 2012

Realmuto, V. J., Abrams, M. J., Buongiorno, M. F., and Pieri, D. C.: The use of multispectral thermal infrared image data to estimate the sulfur dioxide flux from volcanoes: A case study from Mount Etna, Sicily, 29 July 1986, J. Geophys. Res., 99, 481–488, 1994.

Roderick, M., Smith, R. C. G., and Ludwick, G.: Calibrating long term AVHRRderived NDVI imagery, Remote Sens. Environ., 58, 1–12, 1996.

Robock, A.: Volcanic Eruptions and Climate, Rev. Geophys., 38, 191–219, 2000.

Rouse, J. W., Haas, R. H., Schell, J. A., and Deering, D. W.: Monitoring vegetation systems in the Great Plains with ERTS, Third ERTS Symposium, NASA SP-351 I, 309–317, 1973.

Theys, N., Campion, R., Clarisse, L., Brenot, H., Van Gent, J., Dils, B., Corradini, S., Merucci, L., Coheur, P.-F., Van Roozendael, M., Hurtmans, D., Clerbaux, C., Tait, S., and Ferrucci, F.: Volcanic SO_2 fluxes derived from satellite data: a survey using OMI, GOME-2, IASI and MODIS, Atmos. Chem. Phys. Discuss., in press, 2012.

Volz, F. E.: Infrared optical constants of ammonium sulfate, Sahara dust, volcanic pumice and fly ash, Appl. Opt., 12, 564–568, 1973.

Watson, I. M., Realmuto, V. J., Rose, W. I., Prata, A. J., Bluth, G. J. S., Gu, Y., Bader, C. E., and Yu, T.: Thermal infrared remote sensing of volcanic emissions using the moderate resolution imaging spectroradiometer, J. Volcanol. Geoth. Res., 135, 75–89, 2004.

Wen, S. and Rose, W. I.: Retrieval of sizes and total masses of particles in volcanic clouds using AVHRR bands 4 and 5, J. Geophys. Res., 99, 5421–5431, 1994.

AMTD
5, 8859–8894, 2012

Table 1. Cubic polynomial relationship coefficients (see Eq. 9) computed for the MODIS-Terra and MODIS-Aqua channels 29, 31 and 32.

Satellite	Band	a_0	a_1	a_2	a_3
Terra	29 (8.6 µm)	−0.0071	0.2911	1.3887	−0.6987
	31 (11 µm)	−0.0223	0.5584	0.6399	−0.1881
	32 (12 µm)	−0.0177	0.4520	0.7869	−0.2360
Aqua	29 (8.6 µm)	−0.0103	0.3360	1.3054	−0.6569
	31 (11 µm)	−0.0222	0.5579	0.6413	−0.1891
	32 (12 µm)	−0.0176	0.4506	0.7886	−0.2364

AMTD
5, 8859–8894, 2012

Table 2. Cubic polynomial relationship coefficients (see Eq. 15) computed for the MODIS-Terra and MODIS-Aqua channels.

Satellite	b_0	b_1	b_2	b_3
Terra	0.0092	1.2376	−0.4005	0.1543
Aqua	0.0076	1.1886	−0.3293	0.1334

AMTD
5, 8859–8894, 2012

Table 3. SO_2 and ash total masses and mean fluxes (v is the wind speed used) for the two MODIS test case images. All the results have been obtained considering only the plume over the sea.

Total Mass [t]	3 December 2006 SO_2	23 October 2011 SO_2	23 October 2011 Ash
VPR Procedure	1040	3721	2679
LUT Procedure	1268	3379	3383
Mean Fluxes [$t\,d^{-1}$]	($v = 5\,m\,s^{-1}$)	($v = 12\,m\,s^{-1}$)	($v = 12\,m\,s^{-1}$)
VPR Procedure	5139	34 593	19 690
LUT Procedure	6099	34 682	25 050

AMTD
5, 8859–8894, 2012

Table 4. Plume altitude variation, plume altitude and plume temperature for the two test cases.

Plume Altitude variation [m]	3 December 2006 Z_p [km]	3 December 2006 T_p [K]	23 October 2011 Z_p [km]	23 October 2011 T_p [K]
−1000	2.75	271.8	4.5	264.6
−500	3.25	269.2	5	261.3
0	3.75	265.9	5.5	257.5
+ 500	4.25	262.9	6	254.0
+ 1000	4.75	259.8	6.5	250.6

AMTD
5, 8859–8894, 2012

Table 5. SO_2 and ash total masses computed using the VPR procedure for different plume altitudes and temperatures.

Plume Altitude variation [m]	3 December 2006 SO_2 Total Mass [t]	23 October 2011 SO_2 Total Mass [t]	23 October 2011 Ash Total Mass [t]
−1000	1325	5853	3903
−500	1183	4932	3420
0	1040	3721	2679
+ 500	941	3242	2238
+ 1000	859	2961	1983

AMTD
5, 8859–8894, 2012

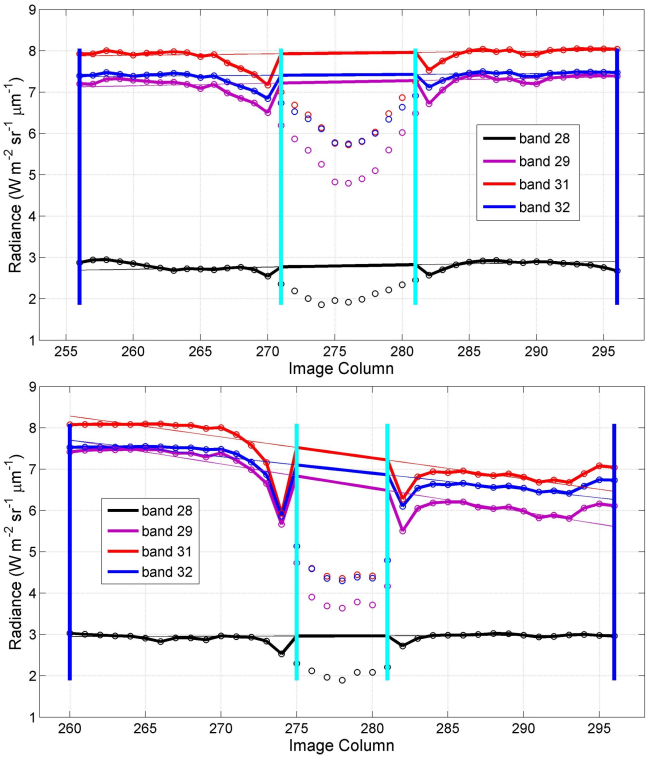

Fig. 1. (a) Radiance of the MODIS bands 28, 29, 31 and 32 in a transect perpendicular to the plume axis over the sea. Circles: measured radiance. Thick lines: radiance if the plume was missing. Thin lines: straight line tangent to valley (plume) obtained considering only the points between the blue and cyan bars. **(b)** Radiance of the MODIS bands 28, 29, 31 and 32 in a transect perpendicular to the plume axis over both sea (left) and land (right). Circles: measured radiance. Thick lines: radiance if the plume was missing. Thin lines: straight line tangent to valley (plume) obtained considering only the points between the blue and cyan bars.

AMTD
5, 8859–8894, 2012

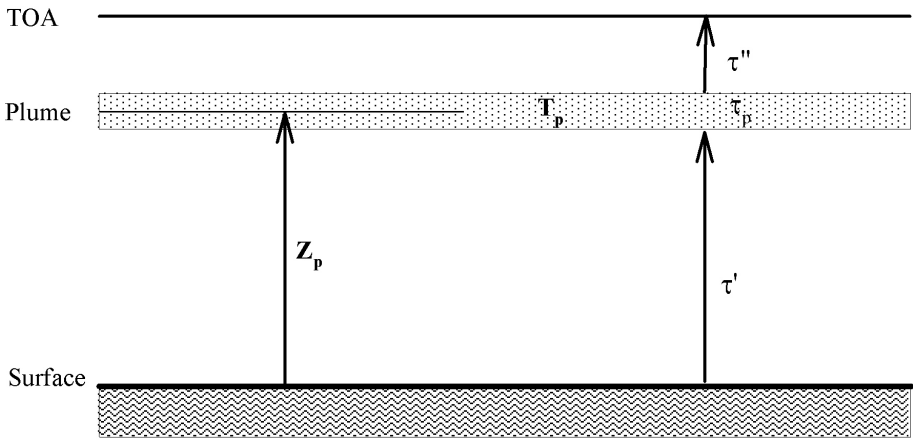

Fig. 2. Schematic representation of the atmospheric model considered.

AMTD
5, 8859–8894, 2012

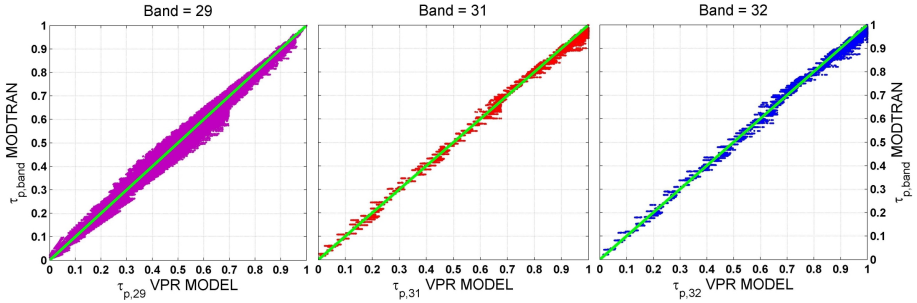

Fig. 3. From left to right: scatter plots of the MODTRAN simulated plume transmittances versus the ones computed using the described procedure, for the channels 29, 31 and 32 respectively. The thick straight line is the bisector.

AMTD
5, 8859–8894, 2012

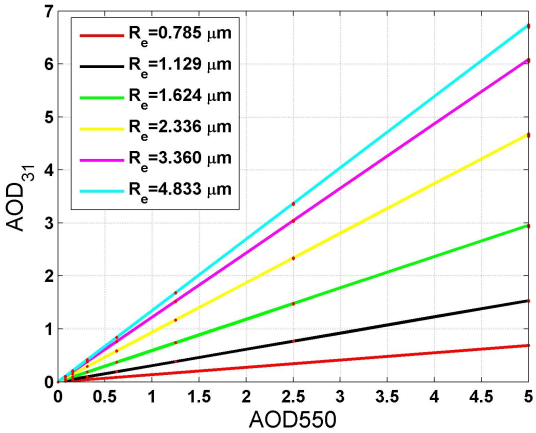

Fig. 4. AOD of the MODIS TERRA band 31 vs. AOD at 550 nm (input MODTRAN parameter). The red points contain all the MODTRAN simulations (12 monthly profiles, 4 plume altitude and 12 viewing angles). The coloured lines are the linear interpolation for the different ash particles effective radius (R_e).

AMTD
5, 8859–8894, 2012

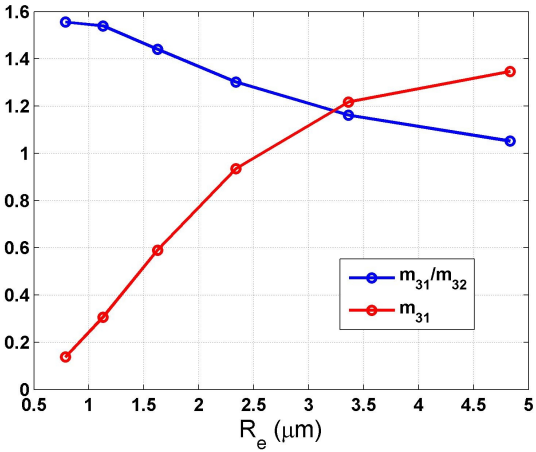

Fig. 5. Trend of TERRA m_{31}/m_{32} and m_{31} slopes versus the effective radius R_e.

AMTD
5, 8859–8894, 2012

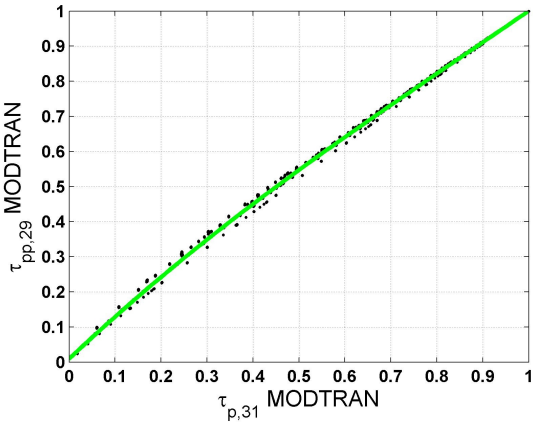

Fig. 6. Plume transmittance of TERRA band 29 vs. plume transmittance of TERRA band 31 considering only ash in the volcanic plume. Green line is a cubic polynomial fit.

AMTD
5, 8859–8894, 2012

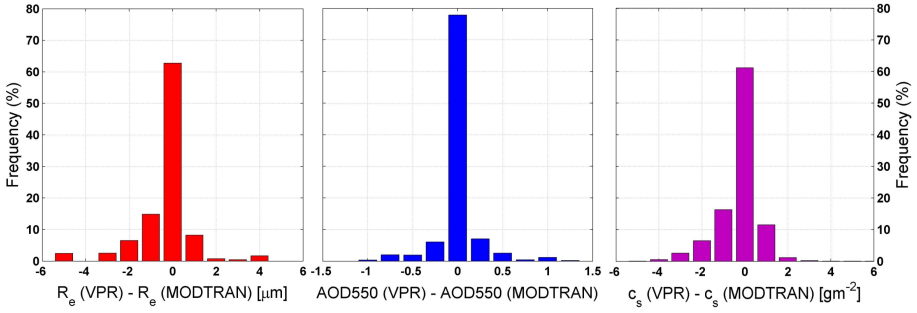

Fig. 7. Frequency (%) of the differences VPR-MODTRAN (MODIS TERRA) for R_e (left), AOD550 (middle) and c_s (right).

AMTD
5, 8859–8894, 2012

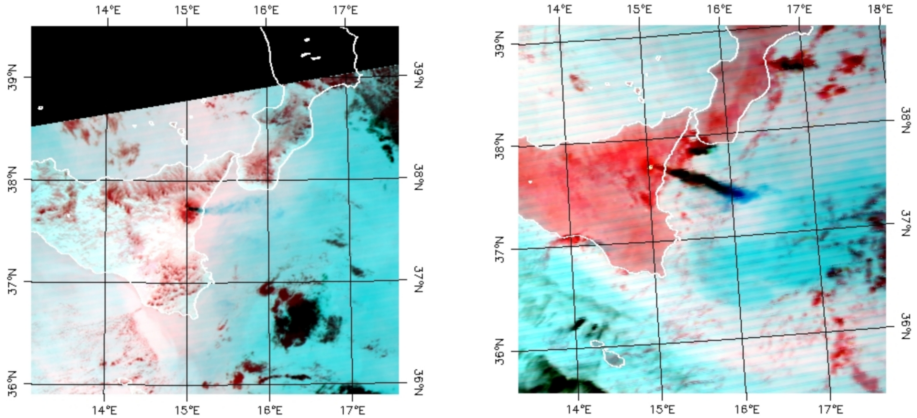

Fig. 8. MODIS RGB image composite (channels 28, 29 and 31) for the two test cases considered: 3 December 2006 – 12:10 UTC – MODIS-Aqua (left) and 23 October 2011 – 21:30 UTC – MODIS-Terra (right).

AMTD
5, 8859–8894, 2012

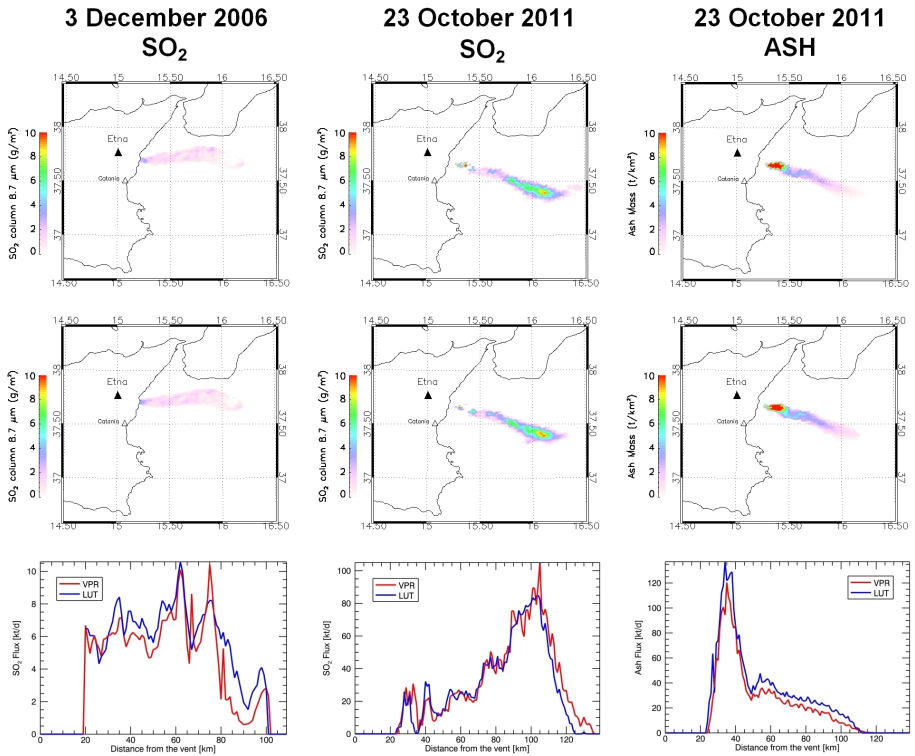

Fig. 9. SO_2 and ash retrievals using the VPR (upper plates) and LUT (middle plates) procedures for the two Etna events considered. The lower plates show the flux comparison.

AMTD
5, 8859–8894, 2012